Research

CrossMark
click for updates

Author for correspondence:
Martín I. Idiart
e-mail: martin.idiart@ing.unlp.edu.ar

THE ROYAL SOCIETY
PUBLISHING

Bounding the plastic strength of polycrystalline voided solids by linear-comparison homogenization techniques

Juan E. Ramos Nervi[1,2] and Martín I. Idiart[1,3]

[1]Departamento de Aeronáutica, Facultad de Ingeniería, Universidad Nacional de La Plata, Avda. 1 esq. 47, La Plata B1900TAG, Argentina
[2]Nucleoeléctrica Argentina S.A., Arribeños 3619, Ciudad Autónoma de Buenos Aires C1429BKQ, Argentina
[3]Consejo Nacional de Investigaciones Científicas y Técnicas (CONICET), CCT La Plata, Calle 8 No 1467, La Plata B1904CMC, Argentina

The elastoplastic response of polycrystalline voided solids is idealized here as rigid-perfectly plastic. Bounds on the macroscopic plastic strength for prescribed microstructural statistics and single-crystal strength are computed be means of a linear-comparison homogenization technique developed by Idiart & Ponte Castañeda (2007 *Proc. R. Soc. A* **463**, 907–924. (doi:10.1098/rspa.2006.1797)). Hashin–Shtrikman (HS) and Self-Consistent (SC) results in the form of yield surfaces are reported for cubic and hexagonal polycrystals with isotropic texture and varying degrees of crystal anisotropy. In all cases, the surfaces are smooth, closed and convex. Improvements over earlier linear-comparison bounds of up to 40% are found at high-stress triaxialities. New HS results can even be sharper than earlier SC results for some material systems. In the case of deficient crystals, the SC results assert that voided aggregates of crystals with four independent systems can accommodate arbitrary deformations, those with three independent systems can dilate but not distort, and those with fewer than three independent systems cannot deform at all. We report the sharpest bounds available to date for all classes of material systems considered.

1. Motivation

Plastic growth of microcavities in polycrystalline ductile solids can be significantly influenced by the

crystallographic and morphological textures of the aggregate (e.g. [1–5]). Theoretical analysis of this process requires micromechanical models that relate the macroscopic stress state with the microscopic plastic deformation in polycrystalline voided systems. A fairly simple approach to the problem consists in idealizing the mechanical response of the individual grains as elastically rigid and plastically non-hardening, and employing homogenization techniques to derive the macroscopic plastic strength in terms of the single-crystal strength and the statistics of the morphology and orientation distributions of the grains and voids (see the monograph by Kocks *et al.* [6]). Owing to their inherent microstructural randomness, cognate polycrystals with the same statistics will not exhibit a single macroscopic response but a range of responses. Therefore, one can either develop estimates that yield a single representative response or derive bounds for the entire range of possible responses. This work is concerned with bounds. Bounds are also useful for two additional reasons: they provide benchmarks to test estimates and they can be used as estimates themselves.

Several homogenization techniques are already available to bound the plastic strength of polycrystalline solids. Their use, however, has so far focused, almost exclusively, on *fully dense* material systems. The simplest bounds are the upper bound of Taylor [7] and the lower bound of Reuss [8], which depend on one-point microstructural statistics only. These elementary bounds have proved useful in the context of high-symmetry polycrystalline solids—like certain face-centred cubic (FCC) solids—where the heterogeneity contrast is low, but as crystal anisotropy increases their predictions diverge and become highly inaccurate. Sharper bounds incorporating higher order statistics were first derived by Dendievel *et al.* [9] and deBotton & Ponte Castañeda [10] making use of the idea of a linear-comparison medium that is optimally selected via a suitably designed variational principle. In particular, the technique of deBotton & Ponte Castañeda [10] allows the use of any linear homogenization approach, such as the Hashin–Shtrikman (HS) or Self-Consistent (SC) approaches, to generate corresponding results for nonlinear polycrystals. Application of these linear-comparison methods to various classes of polycrystalline solids can be found in Willis [11], Nebozhyn *et al.* [12,13], Liu *et al.* [14] and Liu & Ponte Castañeda [15]. These works showed that linear-comparison predictions could improve, sometimes significantly, over the elementary predictions of Taylor and Reuss and served to demonstrate the inconsistency of various theories of polycrystalline plasticity based on *ad hoc* linearization schemes. Idiart & Ponte Castañeda [16,17] later showed that the linear-comparison technique of deBotton & Ponte Castañeda [10] makes implicit use of a relaxation in the variational scheme which weakens the resulting bounds. Eliminating this relaxation leads to sharper bounds at the expense of increasing the computational complexity. The impact of the relaxation on linear-comparison bounds for various cubic and hexagonal systems has been recently assessed by Idiart [18]. Modest differences between relaxed and non-relaxed bounds were observed, with the largest amounts corresponding to polycrystals with deficient slip systems.

The purpose of this work is to assess the performance of the aforementioned homogenization techniques in the context of *voided* polycrystals. Owing to their infinitely large heterogeneity contrast, these are particularly challenging material systems to bound where the various techniques are expected to show large relative deviations. Indeed, it is already known that the elementary bounds become futile in the presence of a vacuous phase—the Reuss bound predicts vanishing strength, while the Taylor bound predicts infinite strength under purely hydrostatic loadings—while linear-comparison bounds remain meaningful. Lebensohn *et al.* [19] have recently reported relaxed linear-comparison bounds of the SC type for (viscoplastic) FCC voided systems. The bounds served to discriminate between two linear-comparison theories of polycrystalline plasticity, but were quite far from predictions obtained by full-field simulations. More recently, Idiart & Ramos Nervi [20] have reported linear-comparison bounds for the hydrostatic strength of cubic systems which confirm that the relaxation can have a significant impact in the presence of a voided phase. Here, linear-comparison bounds of the HS and the SC types[1] are reported for cubic and hexagonal voided polycrystals with isotropic texture

---

[1]Strictly, the use of the HS approach provides bounds for the entire class of polycrystals with prescribed one- and two-point statistics, while the use of the SC approach provides bounds for the subclass of polycrystals that realize the linear SC scheme.

and varying degrees of crystal anisotropy, subject to axisymmetric loading conditions. Because the analysis treats the voided and crystalline phases on an equal footing, the results should be relevant for material systems with intergranular porosity; intragranular porosity should be treated differently (e.g. [21,22]). Special attention is paid to the interplay between crystallinity, porosity and the impact of variational relaxations on the bounds. The sections that follow give a brief summary of the relevant techniques and conclude with a presentation and discussion of representative results.

2. The polycrystalline solid model

Polycrystals are idealized here as random aggregates of perfectly bonded single crystals (i.e. grains) and voids. Individual grains and voids are assumed to be of a similar size, much smaller than the specimen size and the scale of variation of the applied loads. Furthermore, the aggregates are assumed to have statistically uniform and ergodic microstructures.

Plasticity is most conveniently studied by adopting an Eulerian description of motion; the ensuing analysis thus refers to the *current* configuration of the aggregate at a generic stage of deformation. Let the grain orientations take on a set of N discrete values, characterized by rotation tensors $\mathbf{Q}^{(r)}$ ($r = 1, \ldots, N$). All grains with a given orientation $\mathbf{Q}^{(r)}$ occupy a disconnected domain $\Omega^{(r)}$ and are collectively referred to as 'phase' r. Similarly, all voids occupy a disconnected domain $\Omega^{(0)}$ and are collectively referred to as 'phase' 0. The domain occupied by the polycrystal is then $\Omega = \cup_{r=0}^{N} \Omega^{(r)}$.

Grains ($r = 1, \ldots, N$) are assumed to individually deform by multi-glide along K slip systems following a rigid-perfectly plastic response. In accordance with standard crystal plasticity theory, their *strength domains* are given by the convex sets

$$P^{(r)} = \left\{ \boldsymbol{\sigma} : |\boldsymbol{\sigma} \cdot \boldsymbol{\mu}_{(k)}^{(r)}| \leq \tau_0^{(k)}, \ k = 1, \ldots, K \right\}, \tag{2.1}$$

where $\tau_0^{(k)} > 0$ is the yield strength of the kth slip system in a 'reference' crystal and

$$\boldsymbol{\mu}_{(k)}^{(r)} = \frac{1}{2} \left(\mathbf{n}_{(k)}^{(r)} \otimes \mathbf{m}_{(k)}^{(r)} + \mathbf{m}_{(k)}^{(r)} \otimes \mathbf{n}_{(k)}^{(r)} \right) \tag{2.2}$$

are second-order Schmid tensors with $\mathbf{n}_{(k)}^{(r)}$ and $\mathbf{m}_{(k)}^{(r)}$ denoting the unit vectors normal to the slip plane and along the slip direction of the kth system, respectively, for a crystal with orientation $\mathbf{Q}^{(r)}$. The Schmid tensors of a given phase r are related to corresponding tensors $\boldsymbol{\mu}_{(k)}$ for the 'reference' crystal via $\boldsymbol{\mu}_{(k)}^{(r)} = \mathbf{Q}^{(r)T} \boldsymbol{\mu}_{(k)} \mathbf{Q}^{(r)}$. Note that the Schmid tensors are traceless and therefore the strength domains (2.1) are insensitive to hydrostatic stresses. The boundary $\partial P^{(r)}$ of the set $P^{(r)}$ represents the *yield surface* of phase r. Plastic flow of the grains is governed by the so-called normality rule.

The voided phase ($r = 0$), on the other hand, cannot sustain stress. We characterize this phase as an additional family of 'grains' with

$$P^{(0)} = \{\mathbf{0}\}. \tag{2.3}$$

Volume averages over the aggregate Ω and over each phase $\Omega^{(r)}$ will be denoted by $\langle \cdot \rangle$ and $\langle \cdot \rangle^{(r)}$, respectively. The domains $\Omega^{(r)}$ can be described by a set of characteristic functions $\chi^{(r)}(\mathbf{x})$, which take the value 1 if the position vector $\mathbf{x}$ is in $\Omega^{(r)}$ and 0 otherwise. In view of the microstructural randomness, the functions $\chi^{(r)}$ are random variables that must be characterized in terms of ensemble averages [23]. The ensemble average of $\chi^{(r)}(\mathbf{x})$ represents the one-point probability $p^{(r)}(\mathbf{x})$ of finding phase r at $\mathbf{x}$; the ensemble average of the product $\chi^{(r)}(\mathbf{x})\chi^{(s)}(\mathbf{x}')$ represents the two-point probabilities $p^{(rs)}(\mathbf{x}, \mathbf{x}')$ of finding simultaneously phase r at $\mathbf{x}$ and phase s at $\mathbf{x}'$. Higher order probabilities are defined similarly. Due to the assumed statistical uniformity and ergodicity, the one-point probability $p^{(r)}(\mathbf{x})$ can be identified with the volume fractions—or concentrations—$c^{(r)} = \langle \chi^{(r)}(\mathbf{x}) \rangle$ of each phase r, the two-point probability $p^{(rs)}(\mathbf{x}, \mathbf{x}')$ can be identified with the volume average $\langle \chi^{(r)}(\mathbf{x})\chi^{(s)}(\mathbf{x}') \rangle$, and so on. Note that

$\sum_{r=0}^{N} c^{(r)} = 1$. In describing voided polycrystals, it proves convenient to employ the alternative set of concentrations [19]:

$$f = c^{(0)} \quad \text{and} \quad c_{\mathrm{g}}^{(r)} = \frac{c^{(r)}}{1-f} \quad \text{for } r = 1, \dots, N. \tag{2.4}$$

The microstructural variable f denotes the volume fraction of voids, or *porosity*, in the voided polycrystal, while the rescaled grain concentrations $c_{\mathrm{g}}^{(r)}$ denote the volume fraction of grains with a given orientation $\mathbf{Q}^{(r)}$ within the polycrystalline solid matrix, and are such that $\sum_{r=1}^{N} c_{\mathrm{g}}^{(r)} = 1$. Thus, the set of volume fractions $c_{\mathrm{g}}^{(r)}$ characterizes the *crystallographic texture* of the aggregate surrounding the pores, while the multi-point correlation functions characterize the *morphological texture* of the aggregate and the shape and distribution of the voids.

The macroscopic plastic strength of the polycrystalline aggregate corresponds to the set of stress states that can produce macroscopic plastic flow. By homogenizing the relevant field equations, Bouchitté & Suquet [24] showed that the macroscopic plastic strength can be characterized by an *effective strength domain* defined as

$$\tilde{P} = \{\bar{\boldsymbol{\sigma}} : \exists \boldsymbol{\sigma}(\mathbf{x}) \in \mathcal{S}(\bar{\boldsymbol{\sigma}}) \text{ and } \boldsymbol{\sigma}(\mathbf{x}) \in P^{(r)} \text{ in } \Omega^{(r)}, \ r = 0, \dots, N\}, \tag{2.5}$$

where $\bar{\boldsymbol{\sigma}}$ denote the macroscopic stress states that produce macroscopic plastic flow, $\boldsymbol{\sigma}(\mathbf{x})$ are the underlying microscopic stress fields, and

$$\mathcal{S}(\bar{\boldsymbol{\sigma}}) = \{\boldsymbol{\sigma}(\mathbf{x}) : \operatorname{div}\boldsymbol{\sigma}(\mathbf{x}) = \mathbf{0} \text{ in } \Omega, \ \langle \boldsymbol{\sigma}(\mathbf{x}) \rangle = \bar{\boldsymbol{\sigma}} \} \tag{2.6}$$

is the set of statically admissible stress fields with volume average $\bar{\boldsymbol{\sigma}}$. The effective strength domain depends on the *crystallographic* texture of the polycrystal through the set of orientations $\mathbf{Q}^{(r)}$ and concentrations $c_{\mathrm{g}}^{(r)}$, on the *morphological* texture through the ensemble averages of the characteristic functions $\chi^{(r)}(\mathbf{x})$ of the domains $\Omega^{(r)}$, and on the porosity through f. Note that convexity of the sets $P^{(r)}$ implies convexity of $\tilde{P}$. The boundary $\partial\tilde{P}$ of the set $\tilde{P}$ represents the *effective yield surface* of the polycrystalline voided solid, surface that we seek to bound.

3. Linear-comparison bounds and their relaxations

Outer bounds on the effective strength domain (2.5) are obtained here by means of the linear-comparison technique given in Idiart & Ponte Castañeda [16,17]. This section follows the presentation given by Idiart [18] adapted to the case of voided polycrystals. The main idea behind the technique is to introduce a comparison polycrystal with the same microstructural domains $\chi^{(r)}$ as the original polycrystal but with a linear stress–strain-rate local response characterized by a positive-semi-definite,[2] symmetric compliance tensor $\mathbb{S}^{(r)}$. A judicious use of the Legendre transform then generates the bound

$$\tilde{P} \subset \tilde{P}_{+} = \{\bar{\boldsymbol{\sigma}} : \tilde{u}_0(\bar{\boldsymbol{\sigma}}; \mathbb{S}^{(1)}, \dots, \mathbb{S}^{(N)}) \le v(\mathbb{S}^{(1)}, \dots, \mathbb{S}^{(N)}), \ \forall \mathbb{S}^{(r)} \ge 0 \quad (r = 1, \dots, N)\}, \tag{3.1}$$

where

$$\tilde{u}_0(\bar{\boldsymbol{\sigma}}; \mathbb{S}^{(1)}, \dots, \mathbb{S}^{(N)}) = (1-f) \min_{\boldsymbol{\sigma} \in \mathcal{S}^*(\bar{\boldsymbol{\sigma}})} \sum_{r=1}^{N} c_{\mathrm{g}}^{(r)} \left\langle \frac{1}{2} \boldsymbol{\sigma} \cdot \mathbb{S}^{(r)} \boldsymbol{\sigma} \right\rangle^{(r)}, \tag{3.2}$$

$$v(\mathbb{S}^{(1)}, \dots, \mathbb{S}^{(N)}) = (1-f) \sum_{r=1}^{N} c_{\mathrm{g}}^{(r)} v^{(r)}(\mathbb{S}^{(r)}) \tag{3.3}$$

and

$$v^{(r)}(\mathbb{S}) = \sup_{\boldsymbol{\sigma} \in P^{(r)}} \frac{1}{2} \boldsymbol{\sigma} \cdot \mathbb{S}\boldsymbol{\sigma}. \tag{3.4}$$

---

[2] Positive-semi-definiteness of a fourth-order tensor $\mathbb{S}$ will be indicated by the inequality $\mathbb{S} \ge 0$.

In these expressions, $\tilde{u}_0$ represents the effective stress potential of the linear-comparison polycrystal, while the functions $v^{(r)}$ represent a measure of the nonlinearity of the local stress–strain-rate plastic relation. The set $\mathcal{S}^* \subset \mathcal{S}$ denotes the subset of statically admissible stress fields with zero traction on the surfaces $\partial \Omega^{(0)}$ of the voids. The boundary of $\tilde{P}_+$ represents a surface in the space of macroscopic stresses that bounds from outside the effective yield surface of the polycrystalline voided solid; it can be written as

$$\partial \tilde{P}_+ = \left\{ \bar{\sigma} : \bar{\sigma} = \Lambda \bar{\Sigma} \text{ with } \|\bar{\Sigma}\| = 1 \text{ and } \Lambda = \inf_{\mathbb{S}^{(r)} \geq 0} \left(\frac{\tilde{u}_0(\bar{\Sigma}; \mathbb{S}^{(1)}, \dots, \mathbb{S}^{(N)})}{v(\mathbb{S}^{(1)}, \dots, \mathbb{S}^{(N)})} \right)^{-1/2} \right\}, \quad (3.5)$$

where $\| \cdot \|$ denotes the Euclidean norm of a tensor. The reader is referred to the work of Idiart & Ponte Castañeda [16]—§4b—for details on the derivation.

Thus, to compute the outer bound (3.5), we must determine the effective stress potential $\tilde{u}_0$ in terms of the statistics of $\chi^{(r)}$ and the phase compliance tensors $\mathbb{S}^{(r)}$. In view of the local linearity, this potential can be written as

$$\tilde{u}_0(\bar{\sigma}; \mathbb{S}^{(1)}, \dots, \mathbb{S}^{(N)}) = \tfrac{1}{2} \bar{\sigma} \cdot \tilde{\mathbb{S}}(\mathbb{S}^{(1)}, \dots, \mathbb{S}^{(N)}) \bar{\sigma}, \quad (3.6)$$

where $\tilde{\mathbb{S}}$ is the effective compliance tensor of the linear-comparison polycrystal. In practice, the tensor $\tilde{\mathbb{S}}$ cannot be computed and it must be bounded from below—in the sense of quadratic forms—so that the set (3.5) still bounds from the outside the effective yield surface of the polycrystals. The results reported in this work make use of the HS lower bound of Willis [23,25], which for voided polycrystals takes the form

$$\tilde{\mathbb{S}} = \left[(1-f) \sum_{r=1}^{N} c_g^{(r)} (\mathbb{S}^{(r)} + \mathbb{S}^*)^{-1} \right]^{-1} - \mathbb{S}^*, \quad (3.7)$$

where $\mathbb{S}^* = \mathbb{Q}_0^{-1} - \mathbb{S}_0$ is Hill's constraint tensor, $\mathbb{S}_0$ is a reference compliance tensor and $\mathbb{Q}_0$ is a microstructural tensor that depends on $\mathbb{S}_0$ and on the 'shape' of the two-point correlation functions $p^{(rs)}(\mathbf{x}, \mathbf{x}')$ for the distribution of the grain orientations within the aggregate—the reader is referred to Willis [23,25] for details. Thus, this bound depends on one- and two-point microstructural statistics and is sharper than the corresponding elementary bound. The reference compliance tensor $\mathbb{S}_0$ must be chosen so that the inequality $\mathbb{S}^{(r)} - \mathbb{S}_0 \geq 0$—in the sense of quadratic forms—holds for $r = 1, \dots, N$. Noting that the optimal tensors $\mathbb{S}^{(r)}$ must be incompressible, a simple choice is

$$\mathbb{S}_0 = \frac{1}{2\mu_0} \mathbb{K}, \quad (3.8)$$

where $\mathbb{K}$ is the standard fourth-order incompressible identity tensor and $(2\mu_0)^{-1}$ is taken to be the smallest eigenvalue of all the tensors $\mathbb{S}^{(r)}$. With the choice (3.8), the surface (3.5) bounds from the outside the yield surface of all polycrystals with prescribed one- and two-point statistics. The result (3.7) also serves to generate bounds for *subclasses* of polycrystals with prescribed statistics. For instance, by choosing

$$\mathbb{S}_0 = \tilde{\mathbb{S}} \quad (3.9)$$

the resulting $\tilde{\mathbb{S}}$ reproduces exactly the so-called SC estimate. This estimate is known to be particularly accurate for polycrystalline solids like the ones considered in this work—see, for instance, Lebensohn *et al.* [26]—but more importantly, it is known to be exact for a special subclass of polycrystals with prescribed one- and two-point statistics, consisting of hierarchical microstructures with widely separated length scales. Therefore, the resulting surface (3.5) bounds from the outside the strength domain of all polycrystals belonging to that particular subclass [13]. It is emphasized that regardless of the choice of $\mathbb{S}_0$, the tensor $\mathbb{Q}_0$ is compressible and therefore $\tilde{\mathbb{S}}$ as given by (3.7) is compressible in the presence of porosity ($f > 0$).

In turn, the computation of the functions $v^{(r)}$ requires the solution of the optimization problem (3.4). Since the sets $P^{(r)}$ are closed convex polyhedra formed by the set of hyperplanes (or facets) in stress space whose equations are given by the equalities in (2.1), the maximum in (3.4) is

always attained at some vertices of those polyhedra. The determination of the vertex sets has been discussed in Idiart [18].

(a) Relaxation

The computation of the bound (3.5) can be simplified by restricting the set of compliance tensors $\mathbb{S}^{(r)}$ to those of the form

$$\mathbb{S}^{(r)} = 2 \sum_{k=1}^{K} \alpha_{(k)}^{(r)} \boldsymbol{\mu}_{(k)}^{(r)} \otimes \boldsymbol{\mu}_{(k)}^{(r)}, \quad \alpha_{(k)}^{(r)} \geq 0, \tag{3.10}$$

where the $\boldsymbol{\mu}_{(k)}^{(r)}$ are the Schmid tensors of the crystalline phase r and the scalar variables $\alpha_{(k)}^{(r)}$ represent slip compliances. This class of compliance tensors arise naturally in the linear-comparison bounds of deBotton & Ponte Castañeda [10]; they facilitate the computation of the function v and the optimization with respect to the linear-comparison properties. As a result of the restriction (3.10), we obtain a weaker bound $\partial \tilde{P}'_+$ such that $\tilde{P}_+ \subset \tilde{P}'_+$.

A further simplification results upon use of the inequality

$$\sup_{\boldsymbol{\sigma} \in P^{(r)}} \frac{1}{2} \boldsymbol{\sigma} \cdot \mathbb{S}^{(r)} \boldsymbol{\sigma} \leq \sum_{k=1}^{K} \alpha_{(k)}^{(r)} \left(\tau_0^{(k)} \right)^2 \tag{3.11}$$

to replace the functions $v^{(r)}$ in (3.5) by the right-hand sides. The sense of the inequality implies that the resulting bound $\partial \tilde{P}''_+$ is such that $\tilde{P}_+ \subset \tilde{P}'_+ \subset \tilde{P}''_+$. This *relaxed* bound agrees exactly with the bound originally derived—following a different route—by deBotton & Ponte Castañeda [10]. Note that the inequality in (3.11) becomes an equality when the total number of slip systems at the single-crystal level is five and all of them are linearly independent. In that case, the bounds $\partial \tilde{P}'_+$ and $\partial \tilde{P}''_+$ coincide.

4. Results for cubic and hexagonal polycrystals

The above linear-comparison bounds are applied here to various classes of polycrystalline voided solids. In all cases, both crystallographic and morphological textures are assumed to be *statistically isotropic*, so that the aggregate exhibits overall plastic isotropy. This amounts to assuming that the two-point correlation functions $p^{(rs)}$ are isotropic and that $c_g^{(r)} = 1/N$ ($r, s = 1, \ldots, N$). In view of the overall isotropy, the effective yield surface can be expressed in terms of the three isotropic stress invariants $\bar{\sigma}_m$, $\bar{\sigma}_e$ and $\bar{\theta}$ defined by

$$\bar{\sigma}_m = \frac{1}{3} \operatorname{tr} \bar{\boldsymbol{\sigma}}, \quad \bar{\sigma}_e = \sqrt{\frac{3}{2} \bar{\boldsymbol{\sigma}}_{\mathrm{d}} \cdot \bar{\boldsymbol{\sigma}}_{\mathrm{d}}} \quad \text{and} \quad \cos(3\bar{\theta}) = \frac{27}{2} \det \left(\frac{\bar{\boldsymbol{\sigma}}_{\mathrm{d}}}{\bar{\sigma}_e} \right), \tag{4.1}$$

where $\bar{\boldsymbol{\sigma}}_{\mathrm{d}}$ is the deviatoric part of $\bar{\boldsymbol{\sigma}}$. The stress invariant $\bar{\theta}$ is a homogeneous function of degree zero in $\bar{\boldsymbol{\sigma}}$ and characterizes the 'direction' of the macroscopic shear stress in deviatoric space: the particular values $\bar{\theta} = 0$ and $\bar{\theta} = \pi/6$ correspond to axisymmetric and simple shear loadings, respectively. However, the variation of $\tilde{\sigma}_0$ with $\bar{\theta}$ is not studied here and only the case of axisymmetric loadings is considered. Finally, the stress triaxiality is defined as the ratio $\bar{X}_\sigma = \bar{\sigma}_m / \bar{\sigma}_e$.

The results presented below correspond to 200 crystal orientations ($N = 200$) prescribed according to a Sobol sequence [27] in order to generate textures as close as possible to isotropy (see, for instance, Lebensohn *et al.* [19]). In any event, the exact same set of orientations were used for all computations so that comparisons between the different bounds are meaningful. The various algorithms employed in the calculations have been described in Idiart [18]. Henceforth, non-relaxed bounds of the HS and SC types are labelled HS and SC, respectively, while their relaxed versions, following from (3.11), are denoted by double-primed labels. The non-relaxed bounds reported below make use of compliance tensors of the form (3.10); the work of Idiart [18]

for fully dense polycrystals showed that the loss resulting from this restriction on the class of admissible compliances is marginal.

(a) Cubic polycrystals

Results are reported here for polycrystalline solids with three types of cubic crystals: FCC, body-centred cubic (BCC) and ionic crystals.

We assume the FCC crystals deform by plastic slip on four slip planes of the type {111} along three slip directions (per plane) of type ⟨110⟩, which constitute a set of 12 slip systems ($K = 12$). Of these, five are linearly independent, allowing arbitrary plastic deformation of the grains. In turn, we assume the BCC crystals deform by slip along the ⟨111⟩ directions on the {110} and {112} planes—pencil glide along {123} planes is not considered—which constitute a set of 24 slip systems ($K = 24$). Of these, five are linearly independent. Finally, we assume ionic crystals deform by plastic slip on three different families of slip systems: {110}⟨110⟩, {100}⟨110⟩, {111}⟨110⟩. They will be referred to as *A*, *B* and *C* families. The *A* family consists of six systems, among which two are linearly independent and can accommodate only normal components of strain rate—relative to the cubic axes of the crystal. The *B* family consists of six systems, among which three are linearly independent and can only accommodate shear components of strain rate—relative to the cubic axes of the crystal. Because of the orthogonality of the *A* and *B* systems, the two families together provide five independent slip systems so that a general isochoric deformation can be accommodated. The *C* family, in turn, consists of the same 12 slip systems of an FCC crystal. Thus, the three families together consist of 24 slip systems ($K = 24$).

Figure 1 shows bounds for the yield surface of the various cubic solids with a yield strength τ_0 for all slip systems and a moderate porosity level ($f = 0.05$). It is observed that the elementary Taylor bound produces an open cylindrical surface parallel to the axis of hydrostatic stress, while the HS and SC bounds produce smooth, closed and convex surfaces lying within the Taylor surface, as expected. Note that the smoothness is a consequence of the assumed isotropic texture. The main observation in the context of this figure, however, is that the variational relaxation has an appreciable detrimental impact on the linear-comparison bounds in all cases considered. The global impact can be quantified by comparing the norms of the enclosed 'elastic' domains. It is found to be modest in FCC and ionic solids (approx. 15%) but larger in the BCC solid (approx. 25%).[3] However, the impact varies widely with stress triaxiality. Indeed, the impact observed on the bounds for the shear strength is less than 2% in FCC and BCC solids, and approximately 7% in the ionic solid, while for the hydrostatic strength it is approximately 22% in the FCC solid, approximately 29% in the ionic solid and approximately 40% in the BCC solid. In any case, the impact can be significantly larger than that previously observed by Idiart [18] in fully dense polycrystalline solids. In addition, it is seen that the differences between the corresponding non-relaxed bounds for FCC and BCC solids are larger than those between their relaxed counterparts. Thus, the relaxation seems to reduce the sensitivity of the bounds to matrix crystallinity.

More striking, however, is the fact that the non-relaxed HS bounds are sharper than the fully relaxed SC″ bounds above a certain stress triaxiality in the BCC and ionic solids, a feature never observed in the context of fully dense systems. Recall that the HS approach provides bounds for the entire class of polycrystals with prescribed one- and two-point statistics, which includes the subclass of polycrystals that realize the SC scheme. Thus, the non-relaxed HS results constitute rigorous upper bounds for all other results, including the SC″ results. This is an indication that the loss resulting from the relaxation (3.11) depends more crucially on material parameters such as heterogeneity contrast than on the number of slip systems of the constituent crystals. It is recalled that linear-comparison techniques like the ones considered in this work are known to give fairly accurate predictions for voided systems under low to moderate stress triaxialities but unrealistically strong predictions under high triaxialities (see, for instance, Lebensohn *et al.* [19]). While the significant improvements found in this work are not expected to render the predictions

---

[3]Percentages correspond to the difference between the relaxed and non-relaxed results relative to the non-relaxed result.
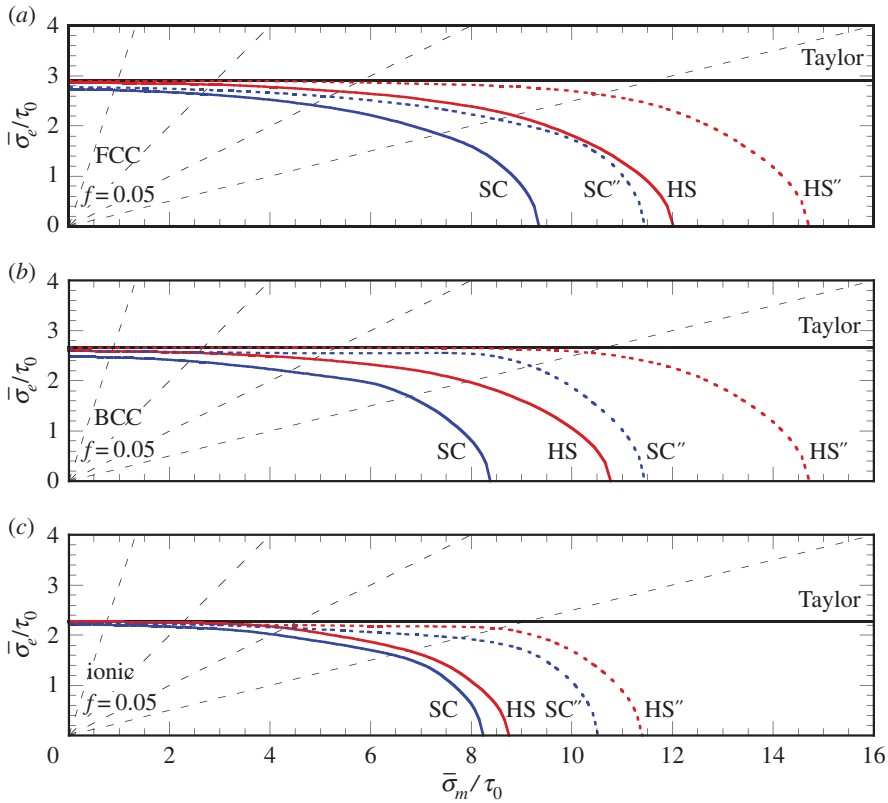
Figure 1. Bounds on the yield surface of isotropic cubic polycrystals with porosity $f = 0.05$, subjected to axisymmetric loadings: (*a*) face-centred cubic solids, (*b*) body-centred cubic solids and (*c*) ionic solids. Relaxed (double-primed) and non-relaxed (unprimed) bounds of the HS and SC type. Dashed lines indicate directions of constant stress triaxialities $\bar{X}_\sigma = 1/3, 1, 2, 4$. (Online version in colour.)

for high triaxialities realistic, they are expected to enlarge the range of stress triaxialities for which the predictions are accurate.

Figure 2 shows the various bounds for ionic solids with a moderate porosity level ($f = 0.05$) and varying degrees of crystal anisotropy. Plots are given for the shear ($\bar{\sigma}_e^c$) and hydrostatic ($\bar{\sigma}_m^c$) plastic strengths as a function of slip contrast between *A*-type and *B*-type systems in ionic solids with infinitely strong C-type systems. We begin by noting that the bounds for the shear strength exhibit similar trends to those previously reported for the fully dense ionic solids—cf. fig. 1 in Idiart [18]—as expected for this porosity level. Thus, the Taylor and HS bounds grow linearly with slip contrast and lie very close to each other for the entire range of plastic anisotropies considered, while the SC bounds—which apply to a subclass of polycrystals—diverge from those bounds exhibiting a different growth and larger differences due to the variational relaxation. On the other hand, the Taylor bound for the hydrostatic strength is infinitely large, and therefore trivial, while the HS and SC bounds for this quantity remain finite as long as *A*-type and *B*-type systems can both deform. Once again, the bounds for the hydrostatic strength exhibit the largest relative differences due to the variational relaxation. However, these differences remain of the same order (approx. 22%) as those reported above for the high-symmetry ionic solid. Additional calculations as a function of porosity [20,28] reveal that the impact of the variational relaxation on these linear-comparison bounds is independent of porosity level. Finally, because the HS bounds grow faster with slip contrast than the SC bounds, the non-relaxed HS bounds for the hydrostatic strength cease to be sharper than the relaxed SC″ bounds above a certain contrast.
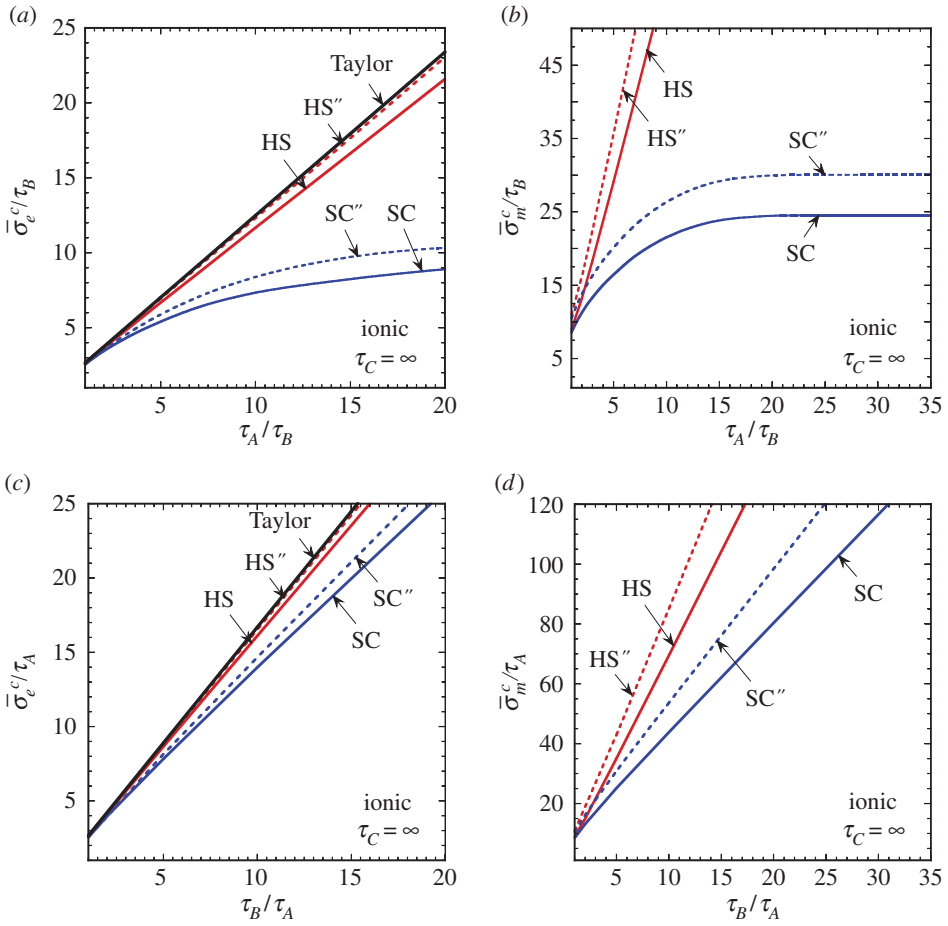
Figure 2. Bounds on the effective strength under shear ($\bar{\sigma}_e^c$) and hydrostatic loadings ($\bar{\sigma}_m^c$) of isotropic ionic polycrystals with porosity $f = 0.05$, as a function of slip contrast. (Online version in colour.)

(b) Hexagonal polycystals

Results are reported here for polycrystalline solids with hexagonal crystal symmetry with ratio $c/a = 1.59$. Plastic deformation is assumed to take place on three sets of slip systems: three basal systems $\{0001\}\langle11\bar{2}0\rangle$, three prismatic systems $\{10\bar{1}0\}\langle11\bar{2}0\rangle$ and 12 first-order pyramidal-$\langle c + a\rangle$ systems $\{10\bar{1}1\}\langle11\bar{2}3\rangle$. They will be referred to as A, B and C families, having flow stresses τ_A, τ_B and τ_C, respectively. Note that the three basal systems and the three prismatic systems supply only two linearly independent systems each, and that the basal systems plus the prismatic systems supply only four linearly independent systems, allowing no straining along the hexagonal crystal axis. On the other hand, the 12 pyramidal systems contain a set of five independent systems. The three families together provide a set of 18 slip systems ($K = 18$).

Figure 3 shows bounds for the yield surface of hexagonal solids with $\tau_A = \tau_B = \tau_C = \tau_0$ and a moderate porosity level ($f = 0.05$). Once again, the linear-comparison bounds produce smooth, closed and convex surfaces that are enclosed by the Taylor surface, as they should, and the relaxation of the function v is seen to have a notorious detrimental impact on these surfaces, especially at large stress triaxialities. Indeed, the overall impact of the relaxation as measured by the norms of the 'elastic' domains is approximately 21%, but the impact on the shear strength is approximately 1% while on the hydrostatic strength is approximately 40%. Moreover, the non-relaxed HS bound is found to be significantly sharper than the relaxed SC″ bound above a certain
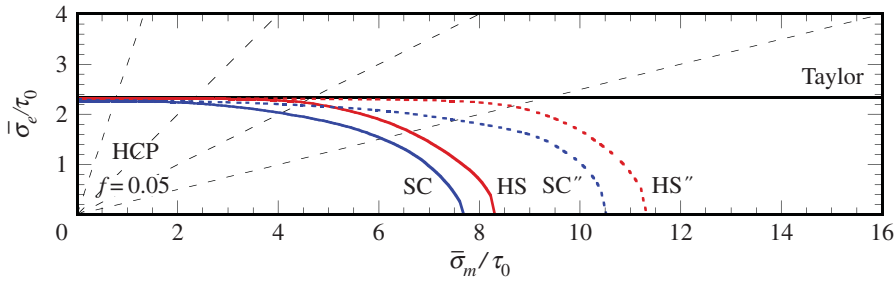
Figure 3. Bounds on the yield surface of isotropic hexagonal polycrystals with porosity $f = 0.05$, subjected to axisymmetric loadings. Relaxed (double-primed) and non-relaxed (unprimed) bounds of the HS and SC type. Dashed lines indicate directions of constant stress triaxialities $\bar{X}_\sigma = 1/3, 1, 2, 4$. HCP, hexagonal closed packed. (Online version in colour.)

stress triaxiality, as already observed in BCC and ionic solids. It should be remarked, however, that because the SC bounds exhibit a lower percolation porosity than the HS bounds, the HS bound cease to be sharper than the SC″ bound at larger porosity levels.

Figure 4 shows the various bounds for hexagonal solids with a moderate porosity level ($f = 0.05$) and varying degrees of crystal anisotropy. Plots are given for the shear ($\bar{\sigma}_e^c$) and hydrostatic ($\bar{\sigma}_m^c$) plastic strengths as a function of slip contrast in solids with $\tau_A = \tau_B \neq \tau_C$ and with $\tau_A \neq \tau_B = \tau_C$. Once again, the bounds for the shear strength exhibit similar trends to those previously reported for the corresponding fully dense solids—cf. fig. 2 in Idiart [18]—as expected for this porosity level. Thus, the Taylor and HS bounds grow linearly with slip contrast and give similar predictions, while the SC bounds diverge from those bounds exhibiting a different growth and giving presumably more realistic predictions. On the other hand, the Taylor bound for the hydrostatic strength is infinitely large, while the HS and SC bounds for this quantity remain finite as long as the three slip systems can deform. The impact of the variational relaxation on the linear-comparison bounds remains on the order of approximately 40% but is found to decrease somewhat with increasing slip contrast. Thus, the effect of the relaxation seems to depend on porosity, crystallography and crystal anisotropy in an intricate manner. Finally, because the HS bounds grow faster with slip contrast than the SC bounds, the non-relaxed HS bounds for the hydrostatic strength cease to be sharper than the relaxed SC″ bounds above a certain contrast.

(c) Polycrystals with deficient slip systems

As the slip contrasts in figures 2 and 4 tend to infinity, the number of linearly independent slip systems in the corresponding constituent crystals becomes deficient, i.e. fewer than five. In this limit, the various bounds for the shear and hydrostatic plastic strengths follow scaling laws of the form $\bar{\sigma}_e^c \sim M^{\gamma_e}$ and $\bar{\sigma}_m^c \sim M^{\gamma_m}$, where M is the relevant slip contrast.

More specifically, for the Taylor bound $\gamma_e = 1$ and γ_m is undefined, while for the HS bounds $\gamma_e = \gamma_c = 1$ independently of crystal symmetry. By contrast, the exponents γ_e and γ_c displayed by the SC bounds are different and do depend on crystal symmetry. These exponents can be expressed in terms of the number J of linearly independent slip systems left in the limit $M \to \infty$ for each case. From the numerical results, it is inferred that $\gamma_e = (4 - J)/2$ and $\gamma_m = (4 - J)(3 - J)/2$. The expression for γ_e is the same as that previously inferred by Nebozhyn et al. [13] for the shear plastic strength of fully dense polycrystals. Indeed, the SC results shown in figure 2c,d for dominant A-type slip ($J = 2$) and in figure 2a,b for dominant B-type slip ($J = 3$) are consistent with exponents $\gamma_e = 1|\gamma_m = 1$ and $\gamma_e = \frac{1}{2}|\gamma_m = 0$, respectively, while those shown in figure 4c,d for dominant basal slip ($J = 2$) and in figure 4a,b for dominant basal+prismatic slip ($J = 4$) are consistent with exponents $\gamma_e = 1|\gamma_m = 1$ and $\gamma_e = 0|\gamma_m = 0$, respectively. Note that the scaling laws are preserved by the relaxation of the function v in the linear-comparison technique. According to these laws, there can be voided aggregates of deficient crystals that can still accommodate
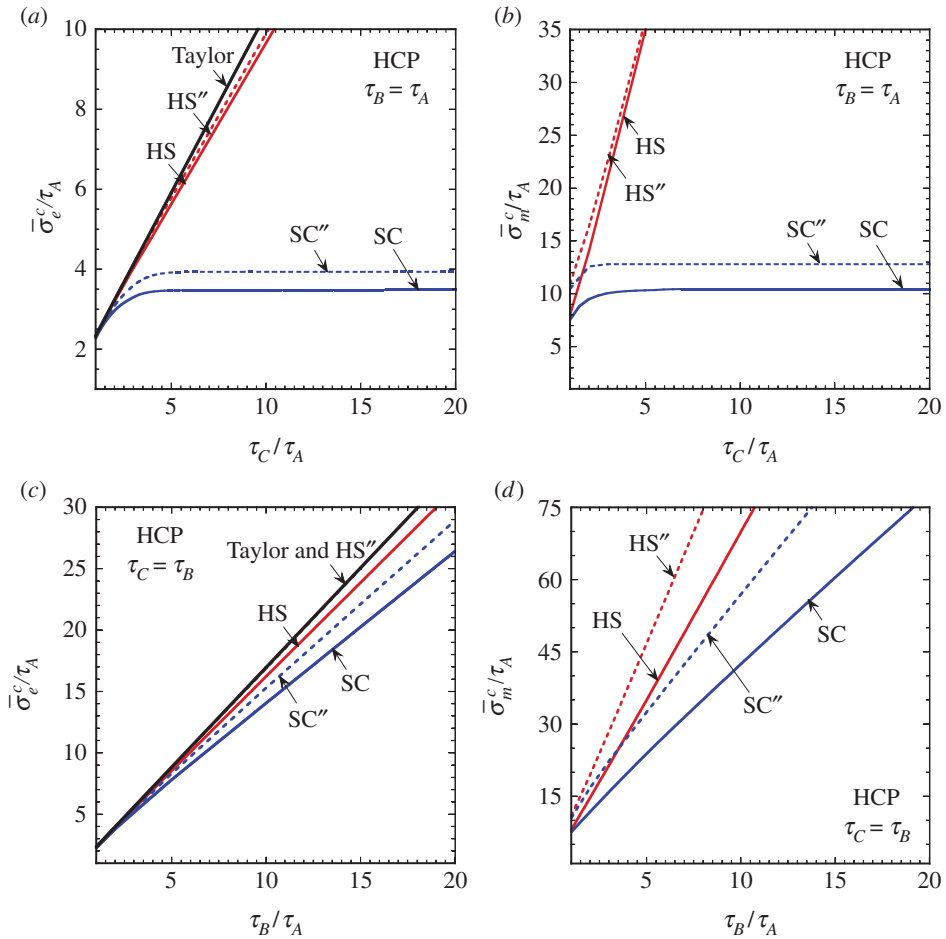
Figure 4. Bounds on the effective strength under shear ($\bar{\sigma}_e^c$) and hydrostatic loadings ($\bar{\sigma}_m^c$) of isotropic hexagonal polycrystals with porosity $f = 0.05$, as a function of slip contrast. (Online version in colour.)

arbitrary macroscopic deformations. However, *spherical* deformations cannot be accommodated by polycrystals with fewer than *three* independent systems, while *deviatoric* deformations cannot be accommodated by polycrystals with fewer than *four* independent systems. In other words, the SC results assert that voided aggregates of crystals with four independent systems can accommodate arbitrary deformations, aggregates of crystals with three independent systems can dilate but not distort, and aggregates of crystals with two independent systems cannot deform at all.

The SC results also predict a substantial change in the interplay between porosity and crystallinity when the crystals are deficient. Indeed, additional calculations [20,28] reveal that when the crystals are not deficient, the bounds for the hydrostatic strength follow a dilute scaling $\bar{\sigma}_m^c \sim f^{-1/2}$. But while the bounds for hexagonal systems undergoing basal+prismatic slip ($J = 4$) also follow this dilute scaling, the bounds for ionic systems undergoing B-type slip ($J = 3$) follow the slower dilute scaling $\bar{\sigma}_m^c \sim f^{-1}$. A change in dilute scaling with material or microstructural properties is typically associated with changes in localization patterns of the underlying strain-rate fields. Linear-comparison techniques are known to have the capacity of capturing certain effects of strain-rate localization on the macroscopic response of isotropic perfectly plastic solids (e.g. [29,30]). From a mathematical standpoint, this capacity stems from the use of extremely anisotropic comparison compliances which allow strain-rate fields in the linear-comparison

medium to localize [31]. This is indeed what produces the above change in dilute scaling with crystallinity (see Ramos Nervi [28] for details). In any event, the capacity to capture such changes, if only approximately, is a remarkable property of linear-comparison techniques which is now confirmed in a more general setting.

Authors' contributions. M.I.I. conceived of the study, designed the study, coordinated the study and drafted the manuscript. J.E.R.M. carried out the calculations, participated in data analysis and helped draft the manuscript. Both authors gave final approval for publication.

Competing interests. We have no competing interests.

References

1. Caré S, Zaoui A. 1996 Cavitation at triple nodes in α-zirconium polycrystals. *Acta Mater.* **44**, 1323–1336. (doi:10.1016/1359-6454(95)00302-9)
2. Hales SJ, Hafley RA. 1998 Texture and anisotropy in Al-Li alloy 2195 plate and near-net-shape extrusions. *Mater. Sci. Eng. A* **257**, 153–164. (doi:10.1016/S0921-5093(98)00834-X)
3. Gray III GT, Bourne NK, Zocher MA, Maudlin PJ, Millett JCF. 2000 Influence of crystallographic anisotropy on the Hopkinson fracture 'spallation' of zirconium. In *Shock compression of condensed matter 1999* (eds MD Furnish, LC Chhabildas, RS Hixson), pp. 509–512. Woodbury, NY: AIP Press.
4. Bache MR, Evans WJ. 2001 Impact of texture on mechanical properties in an advanced titanium alloy. *Mater. Sci. Eng. A* **319–321**, 409–414. (doi:10.1016/S0921-5093(00)02034-7)
5. Millet JCF, Whiteman G, Bourne NK, Gray III GT. 2008 The role of anisotropy in the response of the titanium alloy Ti-6Al-4V to shock loading. *J. App. Phys.* **104**, 073531. (doi:10.1063/1.2991164)
6. Kocks UF, Tomé CN, Wenk H-R. 1998 *Texture and anisotropy*. Cambridge, UK: Cambridge University Press.
7. Taylor GI. 1938 Plastic strain in metals. *J. Inst. Metals* **62**, 307–324.
8. Reuss A. 1929 Calculation of the flow limits of mixed crystals on the basis of the plasticity of the monocrystals. *Z. Angew. Math. Mech.* **9**, 49–58. (doi:10.1002/zamm.19290090104)
9. Dendievel R, Bonnet G, Willis JR. 1991 Bounds for the creep behaviour of polycrystalline materials. In *Inelastic deformation of composite materials* (ed. GJ Dvorak), pp. 175–192. New York, NY: Springer.
10. deBotton G, Ponte Castañeda P. 1995 Variational estimates for the creep behavior of polycrystals. *Proc. R. Soc. Lond. A* **448**, 121–142. (doi:10.1098/rspa.1995.0009)
11. Willis JR. 1994 Upper and lower bounds for nonlinear composite behavior. *Mater. Sci. Eng. A* **175**, 7–14. (doi:10.1016/0921-5093(94)91038-3)
12. Nebozhyn MV, Gilormini P, Ponte Castañeda P. 2000 Variational self-consistent estimates for viscoplastic polycrystals with highly anisotropic grains. *C. R. Acad. Sci. Paris Ser. II* **328**, 11–17.
13. Nebozhyn MV, Gilormini P, Ponte Castañeda P. 2001 Variational self-consistent estimates for cubic viscoplastic polycrystals: the effects of grain anisotropy and shape. *J. Mech. Phys. Solids* **49**, 313–340. (doi:10.1016/S0022-5096(00)00037-5)
14. Liu Y, Gilormini P, Ponte Castañeda P. 2003 Variational self-consistent estimates for texture evolution in viscoplastic polycrystals. *Acta Mater.* **51**, 5425–5437. (doi:10.1016/S1359-6454(03)00409-9)
15. Liu Y, Ponte Castañeda P. 2004 Homogenization estimates for the average behavior and field fluctuations in cubic and hexagonal viscoplastic polycrystals. *J. Mech. Phys. Solids* **52**, 1175–1211. (doi:10.1016/j.jmps.2003.08.006)
16. Idiart MI, Ponte Castañeda P. 2007 Variational principles and bounds for nonlinear composites with anisotropic phases. I. General results. *Proc. R. Soc. A* **463**, 907–924. (doi:10.1098/rspa.2006.1797)
17. Idiart MI, Ponte Castañeda P. 2007 Variational principles and bounds for nonlinear composites with anisotropic phases. II. Crystalline materials. *Proc. R. Soc. A* **463**, 925–943. (doi:10.1098/rspa.2006.1804)

18. Idiart MI. 2012 Bounding the plastic strength of polycrystalline solids by linear-comparison homogenization methods. *Proc. R. Soc. A* **468**, 1136–1153. (doi:10.1098/rspa.2011.0509)

19. Lebensohn RA, Idiart MI, Ponte Castañeda P, Vincent P-G. 2011 Dilatational viscoplasticity of polycrystalline solids with intergranular cavities. *Phil. Mag.* **91**, 3038–3067. (doi:10.1080/14786435.2011.561811)

20. Idiart MI, Ramos Nervi JE. 2014 Bounds on the hydrostatic plastic strength of voided polycrystals and implications for linear-comparison homogenization techniques. *C. R. Mec.* **342**, 25–31. (doi:10.1016/j.crme.2013.11.002)

21. Han X, Besson J, Forest S, Tanguy B, Bugat S. 2013 A yield function for single crystals containing voids. *Int. J. Solids Struct.* **50**, 2115–2131. (doi:10.1016/j.ijsolstr.2013.02.005)

22. Mbiakop A, Constantinescu A, Danas K. 2015 A model for porous single crystals with cylindrical voids of elliptical cross-section. *Int. J. Solids Struct.* **64–65**, 100–119. (doi:10.1016/j.ijsolstr.2015.03.017)

23. Willis JR. 1977 Bounds and self-consistent estimates for the overall moduli of anisotropic composites. *J. Mech. Phys. Solids* **25**, 185–202. (doi:10.1016/0022-5096(77)90022-9)

24. Bouchitté G, Suquet P. 1991 Homogenization, plasticity and yield design. In *Composite media and homogenization theory* (eds G Dal Maso, G Dell'Antonio), pp. 107–133. Basel, Switzerland: Birkhäuser.

25. Willis JR. 1982 Elasticity theory of composites. In *Mechanics of solids* (eds HG Hopkins, MJ Sewell). The Rodney Hill 60th Anniversary Volume, pp. 653–686. Oxford, UK: Pergamon Press.

26. Lebensohn RA, Liu Y, Ponte Castañeda P. 2004 On the accuracy of the self-consistent approximation for polycrystals: comparison with full-field numerical simulations. *Acta Mat.* **52**, 5347–5361. (doi:10.1016/j.actamat.2004.07.040)

27. Sobol IM. 1967 On the distribution of points in a cube and the approximate evaluation of integrals. *USSR Comput. Math. Math. Phys.* **7**, 86–112. (doi:10.1016/0041-5553(67)90144-9)

28. Ramos Nervi JE. In preparation. Plasticidad de materiales policristalinos con porosidad presurizada. M. Eng. thesis, Universidad Nacional de La Plata, Argentina.

29. Idiart MI, Ponte Castañeda P. 2005 Second-order estimates for nonlinear isotropic composites with spherical pores and rigid particles. *C. R. Mec.* **333**, 147–154. (doi:10.1016/j.crme.2004.12.001)

30. Idiart MI, Moulinec H, Ponte Castañeda P, Suquet P. 2006 Macroscopic behavior and field fluctuations in viscoplastic composites: second-order estimates vs full-field simulations. *J. Mech. Phys. Solids* **54**, 1029–1063. (doi:10.1016/j.jmps.2005.11.004)

31. Idiart MI, Willot F, Pellegrini Y-P, Ponte Castañeda P. 2009 Infinite-contrast periodic composites with strongly nonlinear behavior: effective-medium theory versus full-field simulations. *Int. J. Solids Struct.* **46**, 3365–3382. (doi:10.1016/j.ijsolstr.2009.05.009)